ARTICLE

Mitochondrial free cholesterol loading sensitizes to TNF- and Fas-mediated steatohepatitis

Montserrat Marí,[1,4] Francisco Caballero,[2,4] Anna Colell,[2] Albert Morales,[1] Juan Caballeria,[1] Anna Fernandez,[2] Carlos Enrich,[3] José C. Fernandez-Checa,[1,2,*] and Carmen García-Ruiz[1,2,*]

[1] Liver Unit, Institut de Malalties Digestives, Hospital Clínic i Provincial
[2] Department of Experimental Pathology
[3] Department de Biología Cellular, Facultat de Medicina, Universitat de Barcelona
Instituto Investigaciones Biomédicas August Pi i Sunyer (IDIBAPS), Consejo Superior de Investigaciones Científicas, Barcelona, Spain
[4] These authors contributed equally to this work.
*Correspondence: checa229@yahoo.com (J.C.F.-C.); cgrbam@iibb.csic.es (C.G.-R.)

Summary

The etiology of progression from steatosis to steatohepatitis (SH) remains unknown. Using nutritional and genetic models of hepatic steatosis, we show that free cholesterol (FC) loading, but not free fatty acids or triglycerides, sensitizes to TNF- and Fas-induced SH. FC distribution in endoplasmic reticulum (ER) and plasma membrane did not cause ER stress or alter TNF signaling. Rather, mitochondrial FC loading accounted for the hepatocellular sensitivity to TNF due to mitochondrial glutathione (mGSH) depletion. Selective mGSH depletion in primary hepatocytes recapitulated the susceptibility to TNF and Fas seen in FC-loaded hepatocytes; its repletion rescued FC-loaded livers from TNF-mediated SH. Moreover, hepatocytes from mice lacking NPC1, a late endosomal cholesterol trafficking protein, or from obese ob/ob mice, exhibited mitochondrial FC accumulation, mGSH depletion, and susceptibility to TNF. Thus, we propose a critical role for mitochondrial FC loading in precipitating SH, by sensitizing hepatocytes to TNF and Fas through mGSH depletion.

Introduction

Steatohepatitis (SH) represents an advanced stage in the spectrum of fatty liver disease that encompasses alcoholic (ASH) and nonalcoholic steatohepatitis (NASH), two of the most common forms of liver disease worldwide. Although the primary etiology of ASH and NASH is different, these two diseases show almost identical histology characterized by steatosis (macrovesicular > microvesicular), mixed lobular inflammation with scattered PMN leukocytes and mononuclear cells, and hepatocellular cell death due to sensitivity to oxidative stress (Angulo, 2002; Feldstein and Gores, 2005; Tilg and Diehl, 2000). Although fibrosis (generally in zone 3) and other signs, such as occasional acidophil bodies, are not necessary for diagnosis, their presence reflects SH progression (Brunt, 2004). In addition to alcohol or acetaldehyde (Lluis et al., 2003; You and Crabb, 2004) and insulin resistance or hyperinsulinemia (Angulo, 2002; Browning and Horton, 2004; Horton et al., 2002), which promote the hepatic lipid accumulation seen in ASH and NASH, respectively, hyperhomocysteinemia (Ji and Kaplowitz, 2004; Werstuck et al., 2001; Woo et al., 2005) or antiretroviral therapy (Riddle et al., 2001; Williams et al., 2004) stimulate de novo lipid synthesis and hepatic steatosis. The causes for enhanced lipogenesis in these conditions are complex, with the activation of membrane-bound transcription factors SREBP-1c and SREBP-2 playing a prominent role in the synthesis of free fatty acids (FFA) and cholesterol, respectively (Brown and Goldstein, 1997; Browning and Horton, 2004; Horton et al., 2002). In addition, impaired β-oxidation due to mitochondrial dysfunction or carnitine palmitoyl transferase-1 inhibition by malonyl-CoA contributes to the FFA accumulation and storage as triglycerides (TG) in hepatocytes (Abu-Elheiga et al., 2000; McGarry et al., 1977).

The accumulation of lipids in the cytoplasm of hepatocytes, mostly in the form of FFA and TG, is considered the first step in the development of SH. However, SH progression beyond hepatic steatosis usually does not occur in the absence of a second hit that promotes oxidative stress, inflammation, cell death, and fibrosis. In this regard, cytokine overexpression and their membrane receptors have been shown in both ASH and NASH to contribute to hepatocellular apoptosis and SH (Angulo, 2002; Feldstein et al., 2003; Crespo et al., 2001; Iimuro et al., 1997; Yin et al., 1999). For instance, TNF is overexpressed in the liver of obese mice and mediates insulin resistance in both diet-induced and genetic models of obesity (Hotamisligil, 1999; Lin et al., 2002; Uysal et al., 1997). Furthermore, TNF is required for the development of fatty liver by alcohol and subsequent progression to alcohol-induced liver damage (Iimuro et al., 1997; Yin et al., 1999; Xu et al., 2003), and recent findings using mice deficient in both TNF receptor 1 and 2 showed a critical role for TNF signaling in diet-induced NASH (Tomita et al., 2006). However, in addition to TNF, other cytokines also play a role in SH. For instance, a stronger expression of the Fas receptor in hepatocytes has been observed in liver specimens from patients with both ASH and NASH (Feldstein et al., 2003; Ribeiro et al., 2004). Moreover, diet associated hepatic steatosis has been shown to sensitize to Fas-mediated liver injury in mice (Feldstein et al., 2003b). Thus, understanding the mechanisms that determine the susceptibility of steatotic hepatocytes to inflammatory cytokines (e.g., TNF/Fas) is of relevance as it may open the prospect for novel therapeutic strategies for ASH and NASH.

Since FFA, TG, and cholesterol accumulation may coexist in hepatic steatosis, we wondered whether the type rather than the amount of fat determines the susceptibility of the fatty liver

to inflammatory cytokine-mediated hepatocellular apoptosis and SH. Thus, our aim was to address the contribution of individual lipids in the susceptibility of fatty liver to TNF and Fas. Here, using nutritional (feeding a choline-deficient or a hypercholesterolemic diet) and genetic (mice deficient in NPC1, a late endosomal protein involved in intracellular cholesterol trafficking, and obese ob/ob mice) models of hepatic steatosis, we show that free cholesterol (FC) accumulation, but not TG and FFA, sensitizes hepatocytes to TNF- and Fas-induced apoptosis and SH development. This outcome was not mediated by alterations in the apoptotic signaling of TNF, suppression of survival pathways dependent on NF-κB or induction of ER stress due to FC loading. Rather, sensitization to TNF was due to FC accumulation in mitochondria, which resulted in mGSH depletion. Indeed, in vitro mGSH depletion in lean hepatocytes recapitulated the susceptibility seen in FC-loaded hepatocytes, whereas mGSH repletion in vivo rescued FC-loaded livers from TNF-induced SH.

Results

Hepatic steatosis with predominant TG or FC accumulation

In order to examine the contribution of individual lipids in the transition from steatosis to SH, we fed rats a choline-deficient (Lombardi) diet or a sodium cholate-supplemented hypercholesterolemic (HC) diet, for 2–14 days. Livers from rats fed the Lombardi diet for 2 days displayed macrovesicular steatosis, characterized by increased TG levels both in liver and plasma (data not shown), while total cholesterol levels remained unchanged (Figures 1A–1C), as reported previously (Hakamada et al., 1997). Moreover, the levels of phosphatidylcholine (PC) in liver homogenates from Lombardi-fed and chow-fed rats were 41 ± 8 and 52 ± 6 nmol/mg prot after 2 days of feeding and 38 ± 7 and 46 ± 6 nmol/mg prot after 14 days of feeding, with similar phosphatidylethanolamine (PE) levels (33–38 nmol/mg prot). Furthermore, the levels of sphingomyelin, phosphatidylserine, and phosphatidylinositol in liver homogenates from Lombardi-fed rats for 2 or 14 days were similar to those of chow-fed rats (5.2 ± 0.6, 3.1 ± 0.4, and 10.2 ± 1.5 nmol/mg prot, respectively), with no changes in the fatty acid composition (data not shown). Hepatic histology and the lipid profile from rats fed the Lombardi diet supplemented with choline were similar to those of chow-fed rats (data not shown). In contrast, livers from HC diet-fed rats for 2 days exhibited microvesicular steatosis with increased total cholesterol levels in liver and plasma (data not shown), and unchanged TG content (Figures 1A–1C). Hepatic FFA levels increased to a similar extent in both models compared to chow-fed rats (Figure 1D). Feeding a cholesterol enriched diet (2%) for 2 days in the absence of 0.5% sodium cholate did not increase cholesterol levels (Figure S1 in the Supplemental Data available with this article online), requiring longer feeding time (6–8 days) for cholesterol accumulation (data not shown). Furthermore, feeding Lombardi and HC diets increased hepatic SREBP-1c mRNA levels, while the HC diet increased acyl CoA:cholesterol acyl transferase (ACAT) mRNA levels. SREBP-2 and HMGCoA reductase (HMGCoAR) mRNA levels, however, decreased upon HC diet feeding (Figure S2). Rats fed the Lombardi diet displayed increased HMGCoAR mRNA levels (Figure S2). To examine whether this nutritional approach enhanced hepatic FC levels, we stained cultured hepatocytes with filipin, a fluorescent polyene antibiotic, which binds specifically to the 3β-hydroxyl group of sterols (Norman et al., 1972) (Figure 1E). As seen, FC in hepatocytes from chow-fed or Lombardi-fed rats was present mostly in the plasma membrane, while feeding HC diet markedly increased FC levels in plasma membrane and in intracellular sites (Figure 1E). Moreover, the hepatic total cholesterol levels increased gradually over the 14 days of HC diet feeding with FC pool peaking between 1–5 days followed by enhanced cholesteryl ester formation (data not shown). Finally, we examined the histology, lipid profile, and mRNA levels in the livers from Lombardi diet-fed rats for 3 days and then switched to the HC diet for 2 days (L-HC), a condition in which TG and FC accumulation coexist. As seen, this approach resulted in a mixed phenotype with macrovesicular steatosis, increased TG levels, and FC accumulation and changes in SREBP1c, SREBP-2, ACAT, and HMGCoAR mRNA levels (Figures 1A–1E and Figure S2).

FC accumulation sensitizes the liver to TNF- and Fas-mediated SH

Since inflammatory cytokines promote SH (Angulo, 2002; Feldstein and Gores, 2005), we examined the fate of TG- or FC-loaded hepatocytes in response to TNF and Fas. While hepatocytes from Lombardi-fed rats were insensitive to TNF exposure, TNF was cytotoxic to hepatocytes from HC diet-fed rats, inducing apoptotic and necrotic cell death (Figure 2A). Morevoer, TNF induced the release of cytochrome c, caspase-3 activation, and ROS generation in hepatocytes from HC diet-fed rats (Figures 2B–2D). The susceptibility of hepatocytes from HC-fed rats to TNF was prevented by GSH-EE, vitamin E, or BHT treatment (data not shown). TNF or LPS are known to induce in vivo lethal hepatitis after sensitization of the liver with D-galactosamine (Lehmann et al., 1987; Mari et al., 2004). Thus, we assessed the in vivo susceptibility of Lombardi or HC diet-fed rats to LPS challenge. Compared to chow-fed rats, LPS induced minimal liver injury in Lombardi diet-fed rats (Figures 2E–2G), while causing extensive hemorrhagic lesions, clusters of necrotic hepatocytes in HC diet-fed rats (Figures 2E–2G), and inflammatory cell infiltration reflected by myeloperoxidase staining (Figure 2H). Moreover, we tested the effect of a sublethal dose (5 μg/mice, i.p.) (Feldstein et al., 2003b) of the agonistic anti-Fas antibody Jo2 to mice fed the Lombardi or the HC diets. As seen, Jo2 caused significant hepatocellular death and apoptosis, release of serum ALT, and inflammation in HC- or L-HC-fed mice (Figure 2G) with myeloperoxidase staining (data not shown), whereas in Lombardi-fed mice the injury was minimal. Similar findings were observed upon TNF administration (i.v.) to HC-fed rats (data not shown). Consistent with the time-dependent pattern of FC loading, the susceptibility to cytokines translated in hepatocellular death and inflammation is observed after feeding the HC diet for 1–5 days (data not shown). Furthermore, steatotic hepatocytes with TG and FC accumulation from L-HC-fed rats exhibited a similar hepatocellular susceptibility to TNF in vitro or LPS in vivo as HC-fed rats (Figures 2E–2G). Thus, the presence of TG does not alter the susceptibility to TNF or Jo2 caused by FC loading, and this in vivo sensitization contributed to SH.

Diet-induced FC loading, TNF signaling, and ER stress

We examined whether cholesterol loading perturbed TNF signaling by analyzing the activation of NF-κB and the generation

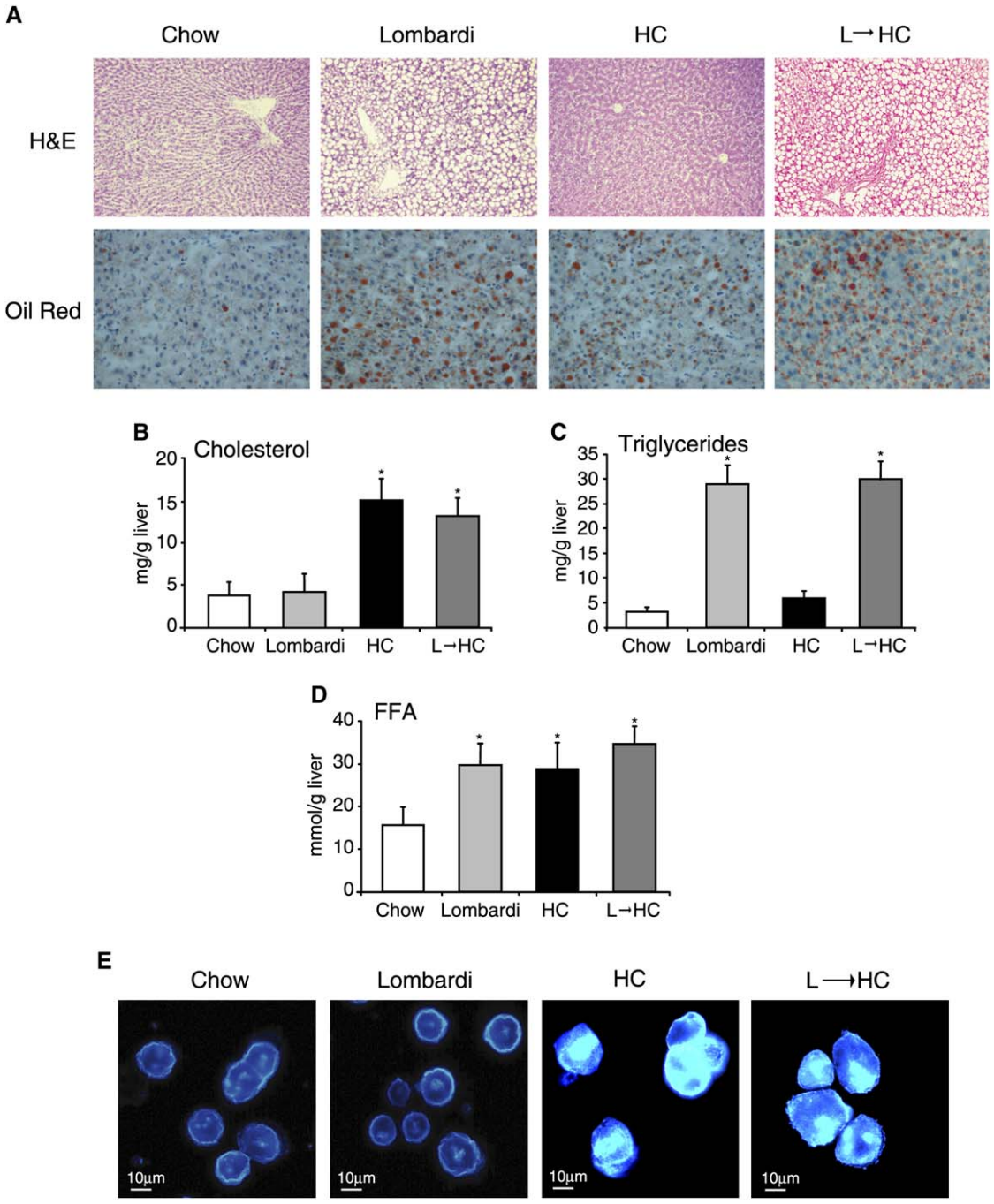

Figure 1. Diet-induced hepatic steatosis

A) Representative hematoxylin and eosin (H&E) (magnification at 10×) or Oil Red O-stained 4-micron sections (magnification at 20×) of liver sections from chow-, Lombardi-, or HC-fed rats for 2 days. L-HC animals were fed Lombardi diet for 3 days plus HC diet for 2 days.

B–D) Hepatic cholesterol, TG, and FFA concentrations were measured in liver homogenate from animals fed the different diets for 2 days. All values are expressed as mean (± SEM), n = 8–12. *$p < 0.05$ versus chow-fed group.

E) Representative fluorescence microscopy of free cholesterol by filipin (0.05 mg/ml) staining of cultured hepatocytes isolated from all groups as described in Experimental Procedures.

of proapoptotic signals that reflect the function of complexes I and II of TNF receptor 1 (TNFR1) signaling (Micheau and Tschopp, 2003). The activation of NF-κB, as the nuclear translocation of p65, and caspase 8, bona fide markers of complexes I and II of TNFR1, respectively, were similar in FC-loaded or lean hepatocytes, as well as in hepatocytes from Lombardi-fed rats (Figures S3A and S3B). Further, the TNF-induced JNK phosphorylation and mitochondrial Bax translocation, which mediate TNF apoptosis, were independent of cholesterol loading (Figures S3C and S3D).

ER stress is known to regulate apoptotic pathways (Breckenridge et al., 2003), and FC trafficking to the ER in macrophages

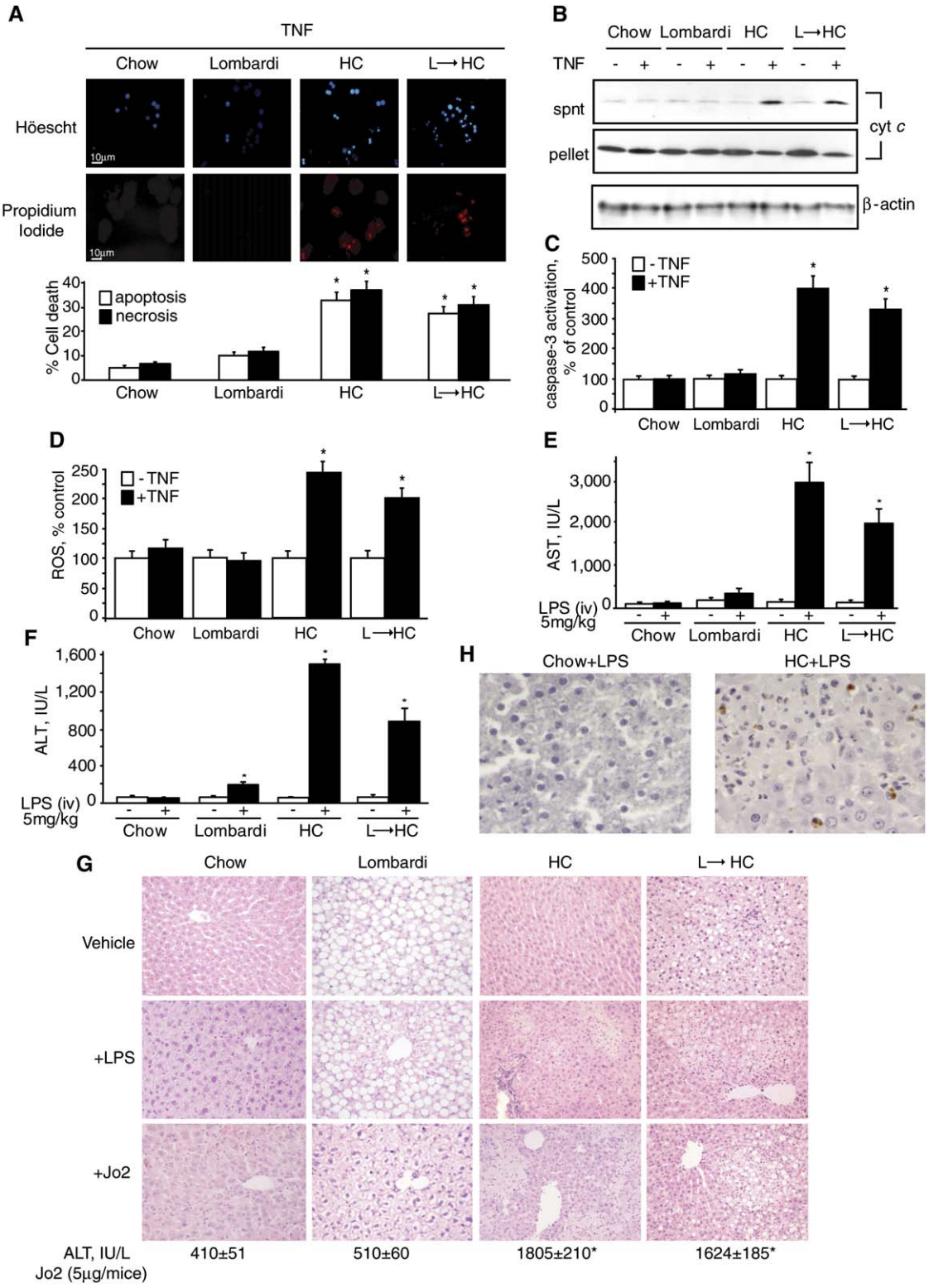

Figure 2. Sensitization of steatotic hepatocytes to TNF

A) Cell death was determined 16 hr after TNF (100 ng/ml) challenge by double staining with Höechst 33258 (10 μM) and propidium iodide (10 μM) to detect apoptotic and necrotic cells, respectively. At least 250 cells in six different high-power fields were counted and expressed as a percentage of total cells (mean ± SD).

B) Cytochrome c release was determined by Western blot 6 hr after TNF challenge in cytosol (spnt) and mitochondria (pellet). β-actin was used as a loading control.

C) 6 hr after TNF treatment, aliquots of cell extracts were prepared for caspase 3 activity using a fluorescent peptide. *$p < 0.001$ versus chow-fed hepatocytes. The data represent the mean ± SEM.

D) ROS were determined 4 hr after TNF challenge in hepatocytes by DCF fluorescence. *$p < 0.01$ versus chow-fed hepatocytes. The data represent the mean ± SEM.

E and F) Serum ALT and AST were determined 24 hr after intravenous LPS injection. Mean ± SEM values are shown, n = 8–12 animals per group. *$p < 0.001$ versus chow-fed group.

has been shown to trigger ER stress and activation of the unfolded protein response (Feng et al., 2003). Thus, we examined whether diet-induced FC accumulation in the liver caused ER stress. Hepatocytes from HC-fed rats exhibited colocalization of filipin with Rab7, a late endosomal marker, and Bip/GRP78, a resident ER chaperone (Figures S3E and S3F), indicating that excess FC derived from diet trafficked from late endosomes to ER. The enrichment of ER in FC observed by filipin staining was confirmed in isolated ER fraction from HC diet-fed rat liver (66% ± 7%, $p < 0.05$) compared to chow control (5.7 ± 0.7 μg/mg protein). Moreover, among the ER-recruited pathways that contribute to cell death include the activation of caspase-12 and the transcription factor CHOP (Breckenridge et al., 2003; Feng et al., 2003). Hepatocytes exposed to tunicamycin/brefeldin A, positive ER stress inducers, exhibited caspase 12 (Figure S3G) and CHOP activation (Figure S3H). In contrast, the levels of CHOP, Bip, or calreticulin were similar in hepatocytes from chow- or HC-fed rats (Figure S3H). In addition, the nuclear content of ATF-4, a downstream effector of the ER-resident protein kinase, PERK, was similar in hepatocytes from chow- or HC-fed rats (data not shown). The extent of caspase-12 activation by FC loading (less pronounced than that caused by tunicamycin/brefeldin A) was insufficient to activate caspase 3 (Figure 2C) and, more important, unchanged by the presence of TNF (Figure S3G). Furthermore, since FC loading in ER can result in ER Ca^{2+} depletion, we analyzed Ca^{2+} release from ER in response to thapsigargin, an inhibitor of ER Ca^{2+} pump (Feng et al., 2003). As seen, the release of Ca^{2+} stores from ER in response to thapsigargin occurred with similar kinetics in hepatocytes from chow- or HC-fed rats with or without TNF exposure (Figure S3I). Together, these findings discard perturbations in the TNF signaling and suggest that ER stress plays a minor role in the sensitization of cholesterol-loaded hepatocytes to TNF.

Diet-induced mitochondrial FC loading depletes mGSH

In addition to the ER, cholesterol also traffics to mitochondria (Soccio and Breslow, 2004). Increased mitochondrial FC accumulation impairs mitochondrial function (Colell et al., 2003; Lluis et al., 2003; Rogers et al., 1980; Rouslin et al., 1982; Yu et al., 2005). Thus, we examined whether the hepatocellular susceptibility to TNF caused by cholesterol accumulation was mediated by mitochondrial FC trafficking. Electron microscopy and Western blot levels of GRP78, Na^+/K^+ATPase α1, Rab5A, and Rab11 of isolated mitochondria indicated insignificant contamination with ER, plasma membrane, and early or recycling endosomes, respectively, in the final mitochondrial fraction from chow- or HC-fed rats (Figures 3A and 3B). Furthermore, the presence of lysosomes, which can participate in cell death pathways, was minimal as the final mitochondrial fraction was de-enriched in acid phosphatase (data not shown). Total cholesterol levels in mitochondria increased gradually only upon HC diet feeding (Figure 3C), in agreement with previous observations (Rogers et al., 1980). However, FC content in mitochondria increased transiently during the first 6 days of HC feeding followed by cholesteryl esters formation (Figure 3D). Furthermore, the distribution of cholesterol esters was 55% ± 5% and 48% ± 7% in the outer mitochondrial membrane for chow-fed and 1 day HC-fed rats, respectively and 38% ± 8% and 31% ± 7% in mitoplasts. To further ensure the accumulation of FC in mitochondria by HC feeding, hepatocytes were stained with filipin and cytochrome c and analyzed by laser confocal microscopy (Figure 3E). FC colocalized with mitochondria as seen by the merged fluorescence of filipin/cytochrome c (Figure 3E). Moreover, the pattern of mitochondrial filipin staining in hepatocytes at day 0 or day 7 after HC feeding was similar (Figure S4), consistent with the free cholesterol content determined biochemically in purified mitochondria (Figure 3D). Since increased levels of cholesterol within biological membranes influence their dynamic properties (Colell et al., 2003; Gimpl et al., 1997; Rouslin et al., 1982), we analyzed the changes in the steady-state fluorescence anisotropy of mitochondria bound dyes to monitor the rotational diffusion freedom of the reported probes with respect to both the rate and the range or extent of the rotational motion (Van Blitterswijk et al., 1981). Hepatic mitochondria from HC-fed rats exhibited higher fluorescence polarization of DPH and TMA-DPH compared to chow or Lombardi diet feeding (Figure 3F), indicating decreased membrane fluidity. Because mGSH plays a critical role in cell defense and TNF susceptibility (Armstrong and Jones, 2002; Colell et al., 1998; Garcia-Ruiz et al., 2003; Lluis et al., 2003) and its transport to mitochondria depends on membrane dynamics (Fernandez-Checa and Kaplowitz, 2005), we examined the levels of mGSH. While cytosol GSH levels were similar in the various dietary groups, mGSH was selectively depleted in hepatocytes from HC-fed rats (Figure 3G). Thus, FC loading in mitochondria decreases mitochondrial membrane fluidity and mGSH levels.

Mitochondrial FC, mGSH depletion, and TNF susceptibility in *NPC1*$^{-/-}$ hepatocytes

We validated the findings in HC-fed rats using another FC loading model. NPC1 is a late endosomal protein involved in the intracellular transport of cholesterol (Liscum, 2000; Soccio and Breslow, 2004), and homozygous mutant *NPC1*$^{-/-}$ mice have been reported to exhibit enhanced hepatic cholesterol content (Beltroy et al., 2005; Erickson et al., 2005). Thus, we assessed the susceptibility of hepatocytes from *NPC1*$^{-/-}$ mice to TNF in relation to the hepatic lipid profile. As seen, the hepatic levels of TG were lower in *NPC1*$^{-/-}$ hepatocytes with unchanged FFA content compared to *NPC1*$^{+/+}$ cells (Figure 4A). However, total cholesterol levels increased 8- to 10-fold (Figure 4A), in agreement with recent observations (Beltroy et al., 2005; Erickson et al., 2005). Moreover, hepatocytes from *NPC1*$^{-/-}$ mice exhibited increased intracellular FC accumulation indicated by filipin staining that colocalized with mitochondria (Figure 4B). The traffic of FC to the ER was defective in *NPC1*$^{-/-}$ hepatocytes (Figure 4C), in agreement with similar findings in macrophages from *NPC1*$^{+/-}$ mice (Feng et al., 2003), consistent with the lack of unfolded protein response and ER stress in *NPC1*$^{-/-}$ hepatocytes based on the levels of PERK, CHOP, and ATF-4 (data not shown). However, as expected from the FC accumulation in hepatocytes (Figure 4B), hepatocytes from

G) Representative H&E slides from rats after the LPS challenge or mice 8 hr after an i.p. injection of Jo2 (5 μg/mouse). H&E-stained sections were photographed on a Zeiss Axioplan using a Nikon DXM1200F digital camera (magnification at 20×). The serum ALT values (IU/L) correspond to the Jo2 treatment, *$p < 0.05$ versus chow-fed mice. **H)** Representative myeloperoxidase staining of liver sections in HC-fed livers challenged with LPS (magnification at 40×).

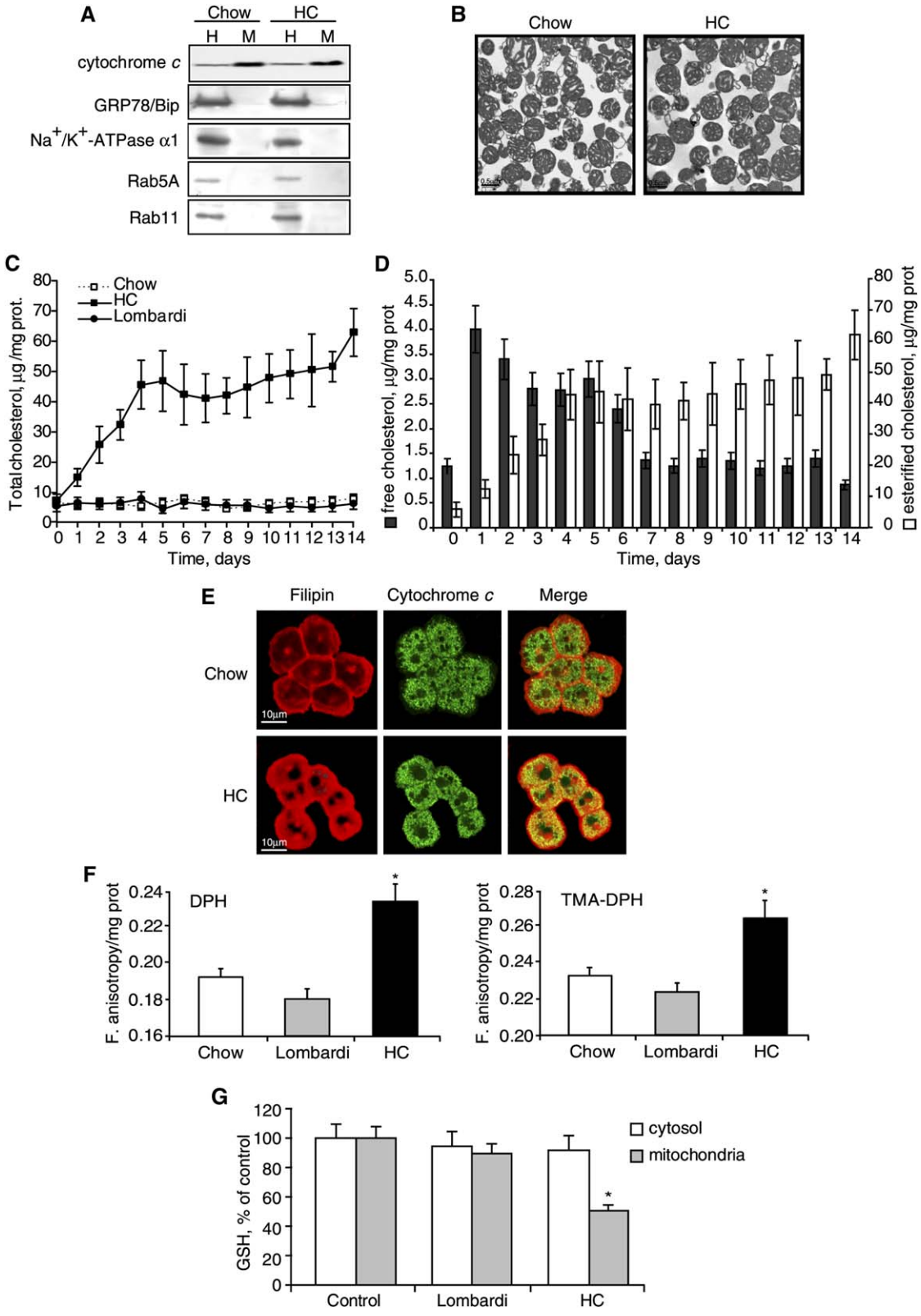

Figure 3. Mitochondrial FC accumulation depletes mGSH

A) Western blot of cytochrome c, GRP78/Bip, Na^+/K^+ATPase α1, Rab5A, and Rab11 in liver homogenates or mitochondrial fraction.

B) Purified mitochondria were fixed and processed for electron microscopy (17,500×).

C and D) Purified rat liver mitochondria were analyzed for the total as well as free and esterified cholesterol content. (**C**) Total cholesterol from chow (n = 8), HC (n = 12), and Lombardi (n = 8) animal feeding are shown. The data represent the mean ± SD. (**D**) Free and esterified cholesterol levels in mitochondria from HC-fed rats were analyzed by HPLC and mean ± SD values are shown.

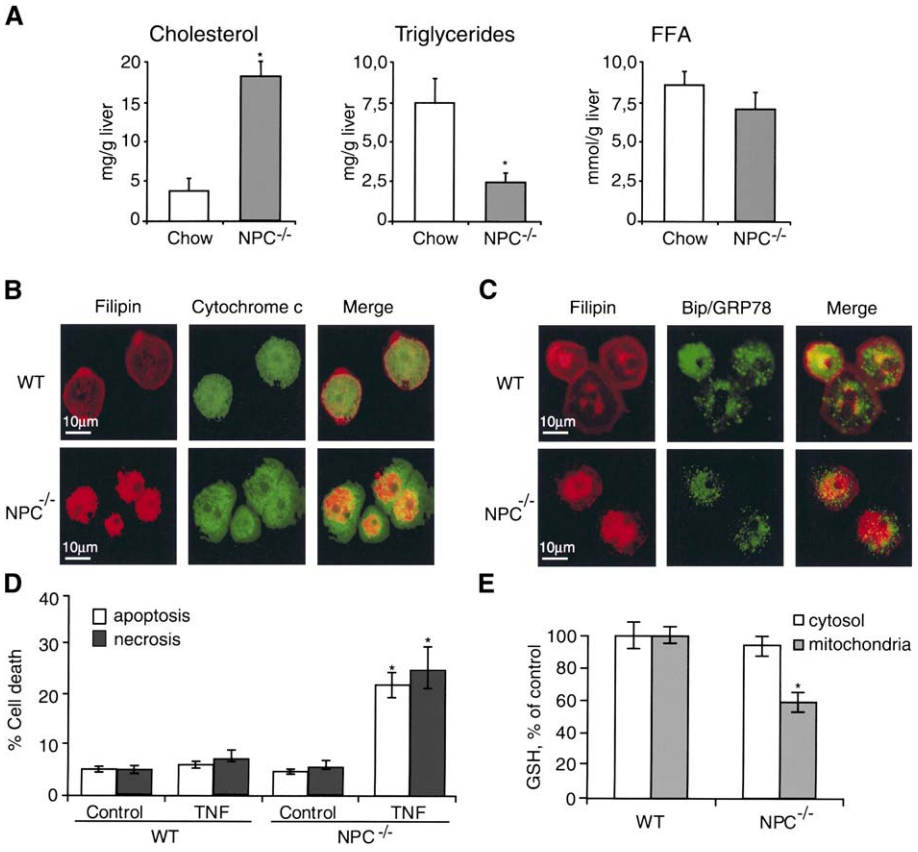

Figure 4. Hepatocytes from *NPC1*$^{-/-}$ mice exhibit mitochondrial FC loading and mGSH depletion

A) Hepatic cholesterol, TG, and FFA concentrations were measured in liver homogenates. All values are expressed as mean (± SEM), n = 5. *p < 0.05 versus chow-fed group.

B and C) Mouse hepatocytes from wild-type or *NPC1*$^{-/-}$ mice were isolated and stained with filipin, mouse anti-cytochrome c, or rabbit anti-Bip/GRP78 followed by the appropriate secondary antibodies. Experiments shown are representative confocal images of three to four different experiments.

D) Cell death was determined by double staining with Höechst 33258 (10 μM) and propidium iodide (10 μM) to detect apoptotic and necrotic cells, respectively. Values are expressed as mean ± SD of at least three experiments. *p < 0.01 versus control WT hepatocytes.

E) compartmentalized GSH from freshly isolated WT and *NPC1*$^{-/-}$ hepatocytes were analyzed by HPLC as described in Experimental Procedures. Results are mean ± SD of at least three experiments. *p < 0.01 versus WT hepatocytes.

NPC1$^{-/-}$ mice exhibited mGSH depletion and susceptibility to TNF (Figures 4D and 4E). Thus these data further confirms the critical role of mitochondrial FC loading in the hepatocellular sensitization to TNF in the absence of increased TG and FFA accumulation.

Hepatocellular TNF sensitization and SH occur if mGSH is low

Next we assessed the causal role of mGSH depletion in the hepatocellular susceptibility to TNF and asked whether mGSH depletion recapitulates the findings of mitochondrial FC loading. We used 3-hydroxy-4-pentenoate (HP) to selectively deplete mGSH pool due to its biotransformation into a Michael electrophyle, which is then conjugated with GSH in the mitochondrial matrix (Shan et al., 1993; Colell et al., 1998; Garcia-Ruiz et al., 2003). As seen, HP-treated hepatocytes exhibited selective mGSH depletion (Figure 5A), with spared cytosol GSH stores. Compared to the resistance of control hepatocytes to TNF, HP treatment sensitized hepatocytes to TNF by a mechanism dependent on caspase-8 activation and oxidative stress (Figure 5B). In addition, mGSH-depleted hepatocytes by HP exhibited enhanced susceptibility to Jo2-mediated cell death compared to untreated cells (28% ± 6% cell death in mGSH-repleted cells and 87% ± 8% cell death in mGSH-depleted hepatocytes, $p < 0.05$). The overgeneration of ROS required both mGSH depletion by HP and TNF, and GSH repletion by the permeable form of GSH, GSH-EE, prevented TNF-induced ROS generation (Figure 5C). Consistent with previous findings on the critical role of acidic sphingomyelinase (ASMase) in TNF-induced hepatocellular apoptosis (Garcia-Ruiz et al., 2003; Osawa et al., 2005), ASMase was necessary for TNF-induced ROS overgeneration (Figure 5D) and cell death (Figure 5E). Furthermore, since NF-κB has been shown to inhibit TNF-induced apoptosis by suppressing ROS (Kamata et al., 2005; Pham et al., 2004), we examined whether mGSH depletion abrogated TNF-induced NF-κB activation. As seen, the kinetics of NF-κB activation by TNF and subsequent gene expression were not affected by mGSH depletion (Figures 5F and 5G). These findings indicate that mGSH determines the hepatocellular susceptibility to TNF through control of mitochondrial ROS stimulation and not by disabling NF-κB-dependent survival pathway.

Furthermore, S-adenosyl-L-methionine (SAM) therapy, which has been shown to fluidize mitochondrial membranes and restore mGSH (Colell et al., 1997; Mari et al., 2004), protected HC-fed rat liver from LPS compared to untreated HC-fed rats, and this effect was accompanied with higher mGSH levels

E) Hepatocytes from chow- or HC-fed rats for 1 day were isolated to examine the colocalization of mitochondria and FC by confocal microscopy using mouse anti-cytochrome c Ab and filipin, respectively.

F) Purified rat liver mitochondria were labeled with DPH or TMA-DPH and fluorescence anisotropy was monitored at 366 nm (emission = 440 nm) using polarizing filters in both excitation and emission planes and normalized per mg of mitochondrial protein. Mean ± SD values from 4 rats/group are shown. *p < 0.01 versus chow-fed group.

G) Compartmentalized GSH from freshly isolated hepatocytes from the various groups were analyzed by HPLC as described in Experimental Procedures. Values are expressed as mean ± SD, n = 12 rats/group. *p < 0.001 versus control hepatocytes.

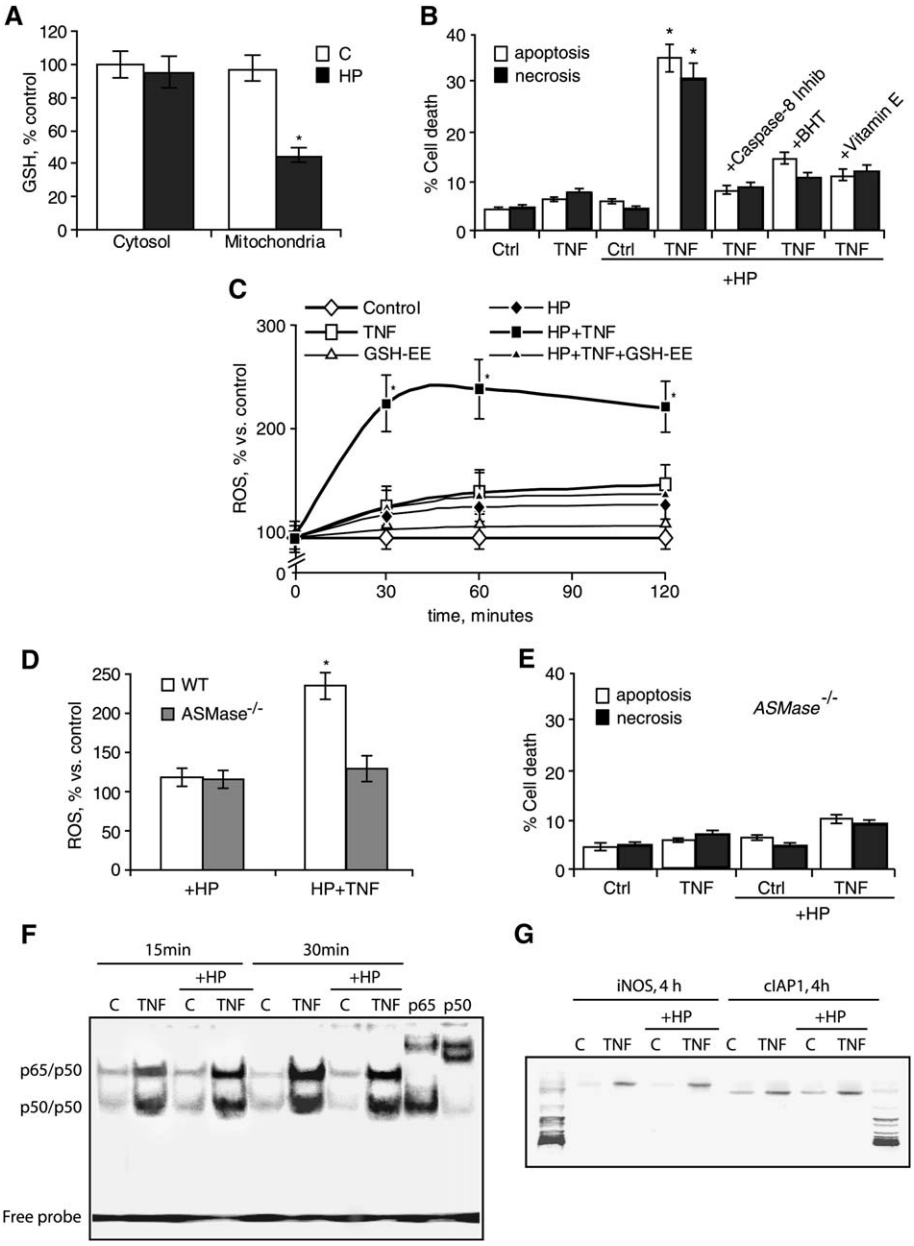

Figure 5. mGSH depletion in vitro by HP sensitizes hepatocytes to TNF

A) GSH compartmentalization in cytosol and mitochondria from hepatocytes treated with HP (0.5 mM) for 5 min. Results are expressed as mean ± SD of at least six experiments. *p < 0.01 versus untreated hepatocytes.

B) Control or HP-treated mouse hepatocytes were exposed to TNF for 16 hr with or without caspase 8 inhibitor, BHT, or vitamin E, as described in Experimental Procedures. Cell death was determined as in Figure 2A. At least 250 cells in six different high-power fields were counted and expressed as a percentage of total cells (mean ± SD). *p < 0.01 versus control.

C) ROS were monitored over time after TNF challenge in hepatocytes. Results are mean ± SD of four experiments. *p < 0.01 versus control.

D) ROS were determined 4 hr after TNF challenge in hepatocytes isolated from wild-type and *ASMase*$^{-/-}$ mice. The data represent the mean ± SD.

E) *ASMase*$^{-/-}$ mouse hepatocytes were exposed to TNF for 16 hr after mGSH depletion by HP. Cell death was determined as in panel (**B**). The data represent the mean ± SD.

F) Representative NF-κB mobility shift assay using nuclear extracts from hepatocytes after TNF exposure.

G) Representative RT-PCR of iNOS and cIAP1, as described in Experimental Procedures.

(Figure 6). The recovery of mGSH occurred between 4–6 hr after SAM treatment (data not shown), suggesting that mGSH normalization protected against LPS-induced SH.

Mitochondrial FC in ASH and NASH and effect of atorvastatin

We next addressed the relevance of these findings in the context of ASH and NASH. Prior evidence using models of alcohol-induced liver damage or HepG2 cells exposed to acetaldehyde showed FC accumulation, mGSH depletion, and hepatocellular susceptibility to TNF (Colell et al., 1997, 1998; Lluis et al., 2003). Moreover, lovastatin pretreatment, which abolished mitochondrial FC accumulation, protected acetaldehyde-exposed HepG2 cells from TNF-induced death through mGSH normalization (Lluis et al., 2003). In contrast to the data in ASH, the role of FC in mitochondria in NASH has not been previously examined. Thus, we analyzed the regulation of FC and mGSH in hepatocytes from obese ob/ob mice. Compared to lean mice, the livers of ob/ob mice had enhanced levels of TG, FFA, and total cholesterol (data not shown). The levels of FC were higher in hepatocytes from ob/ob mice, which colocalized with cytochrome c and Bip/GRP78 (Figures 7A and 7B). As expected from the mitochondrial FC loading, mGSH was depleted in hepatocytes from ob/ob mice with respect to lean mice, whereas the cytosol GSH content remained unchanged (Figure 7C), in agreement with recent findings (Robin et al., 2005). Finally, we examined the therapeutic efficacy of atorvastatin in the regulation of mitochondrial FC loading, mGSH homeostasis and susceptibility to LPS. Atorvastatin therapy to ob/ob mice prevented the accumulation of FC in mitochondria that translated in the normalization of the mGSH pool (Figures 7A and 7C) and restoration of mitochondrial membrane fluidity (data not shown). Moreover, consistent with these

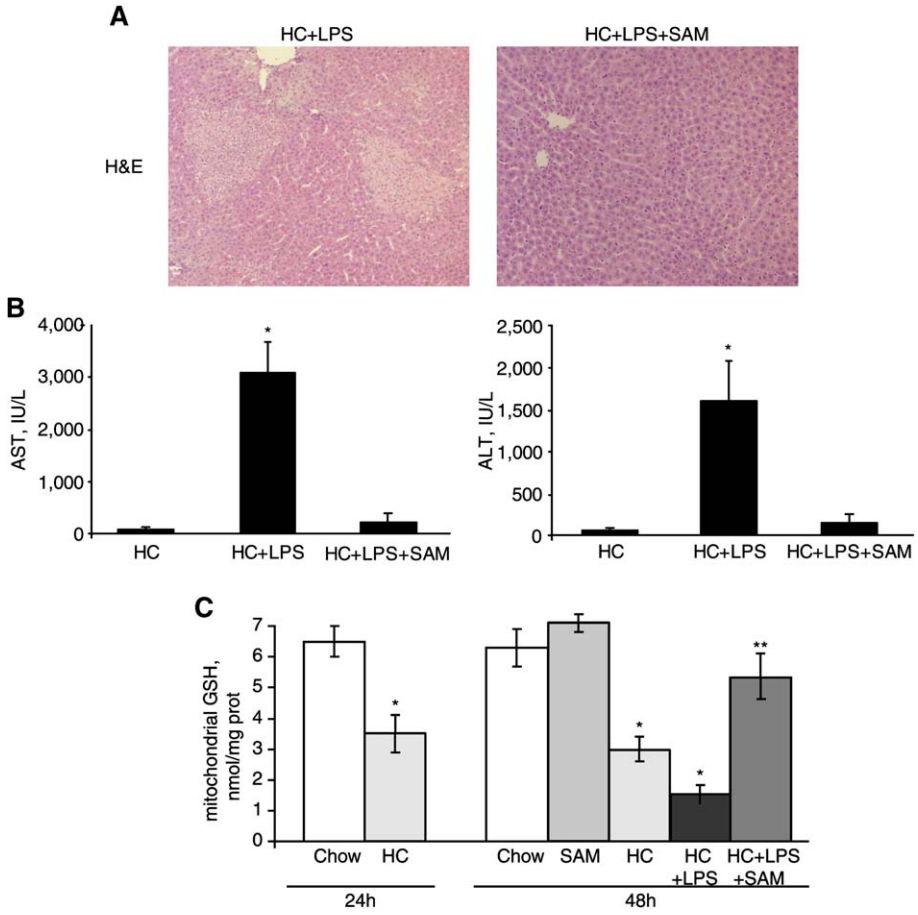

Figure 6. SAM prevents LPS-induced NASH

A) Representative H&E staining of liver samples from HC-fed rats 24 hr after LPS injection plus or minus SAM treatment.

B) Serum ALT and AST 24 hr after intravenous LPS injection plus or minus SAM in HC-fed animals. The data represent the mean ± SEM.

C) GSH levels in mitochondria isolated from chow- or HC-fed rats for 1 day and then treated with LPS plus or minus SAM for 24 hr. Results are expressed as Mean ± SEM, n = 8–12 animals per group. *p < 0.01 versus chow group. **p < 0.05 versus HC+LPS group.

findings, atorvastatin ameliorated the basal signs of SH and prevented the susceptibility of ob/ob mice to LPS-mediated liver injury and inflammation (Figures 7D and 7E). Moreover, atorvastatin treatment did not affect the serum TNF levels upon LPS challenge (2170 ± 180 pg/ml versus 1997 ± 210 pg/ml 90 min after an i.v. injection of LPS in ob/ob mice with or without atorvastatin therapy, respectively). Thus, these data support a potential therapeutic role of statins in NASH development.

Discussion

Discriminating the susceptibility of fatty liver to TNF- and Fas-mediated SH

We used nutritional and genetic models of hepatic steatosis with predominant TG, FFA, and FC accumulation to address whether the type rather than the amount of fat determines the hepatocellular susceptibility to TNF and Fas, which have been shown to contribute to SH (Angulo, 2002; Crespo et al., 2001; Feldstein et al., 2003, 2003b; Ribeiro et al., 2004; Tilg and Diehl, 2000; Tomita et al., 2006). Indeed, defective TNF signaling through both TNF receptor 1 and 2 results in amelioration (but not in prevention) of SH induced by a methionine- and choline-deficient diet (Tomita et al., 2006).

By feeding a HC diet or using *NPC1*$^{-/-}$ mice, we show that FC but not TG or FFA accumulation sensitizes to TNF- and Fas-induced hepatocellular death and inflammation. Previous studies suggested a role for FFA in SH progression and susceptibility to Fas-mediated hepatocellular apoptosis and inflammation (Feldstein et al., 2003, 2003b). However, the role of FFA in this study appears to be minor. First, the accumulation of FFA observed in Lombardi or HC-fed rats was similar with comparable saturated to unsaturated fatty acids profiles in both cases. Second, *NPC1*$^{-/-}$ deficiency resulted in selective cholesterol accumulation with unchanged FFA levels and decreased TG content. Furthermore, in addition to causing hepatic TG accumulation through impaired plasma VLDL secretion, choline deficiency may affect PC synthesis via the CDP-choline pathway. However, the levels of PC in the livers from Lombardi-fed rats were not decreased with respect to those of choline supplemented or chow-fed controls, in agreement with recent observations (Kulinski et al., 2004). In contrast to studies in which choline deficiency was induced along with methionine deprivation, the lack of choline by itself does not seem to limit the synthesis of PC due to the activation of CTP:phosphocholine cytidyltransferase and availability of phosphorylcholine above the K_m for the cytidyltransferase (Kulinski et al., 2004). Consistent with this outcome, choline deficiency did not alter the PC/PE ratio, which has been shown to be a critical determinant of SH progression through maintenance of membrane integrity (Li et al., 2006). Moreover, the nuclear translocation of p65, reflecting the activation of NF-κB, or the cleavage of procaspase 8 by TNF were unaffected by Lombardi diet feeding, suggesting that choline deficiency did not perturb TNF signaling. Thus, although choline deficiency reproduces the TG/FFA accumulation and macrovesicular steatosis observed in liver specimens from morbidly obese subjects and patients with alcoholic liver injury (Mavrelis et al., 1983),

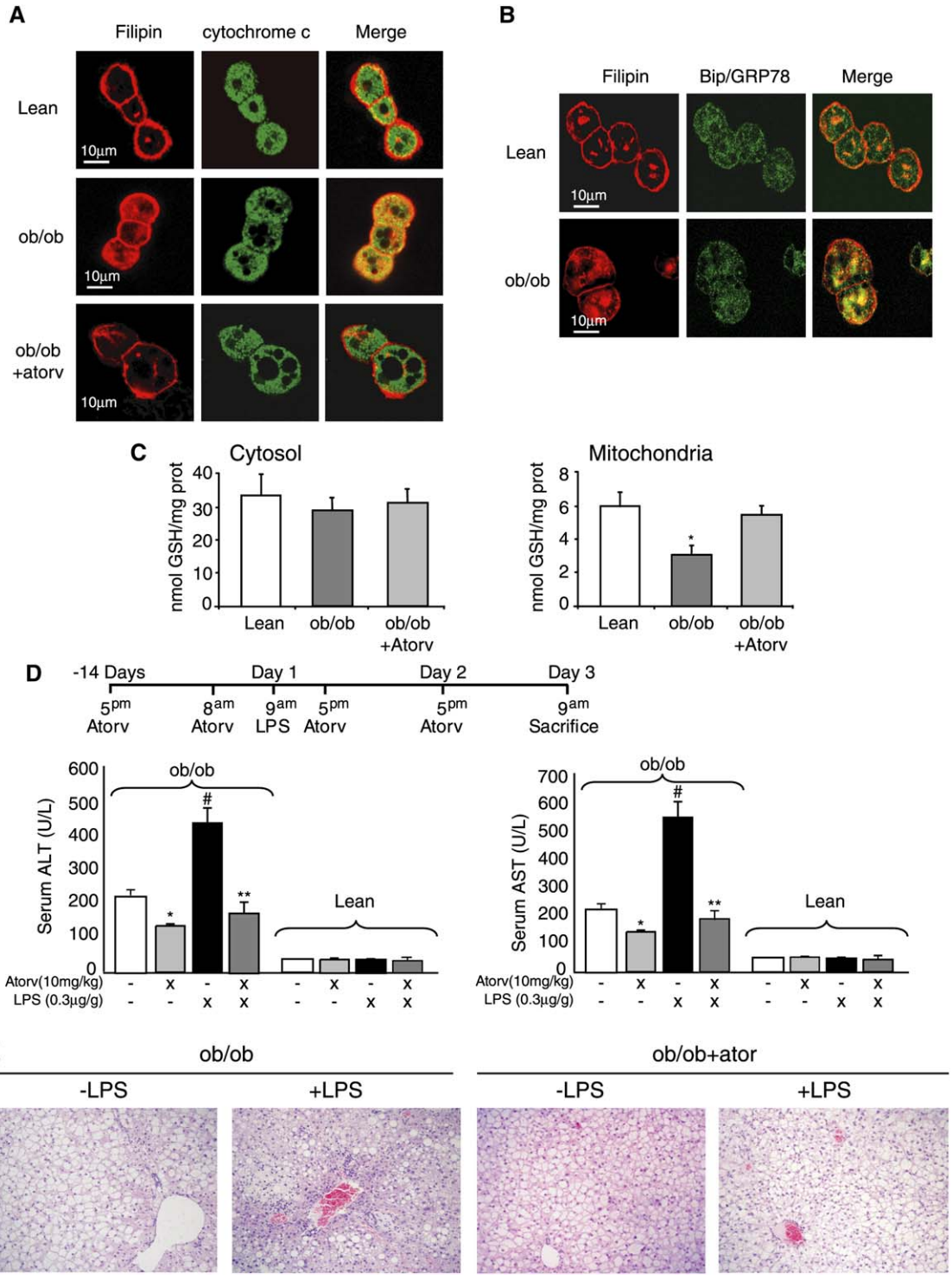

Figure 7. Cholesterol in ob/ob mice and atorvastatin therapy

A and B) Mouse hepatocytes from wild-type or ob/ob mice were isolated and stained with filipin, mouse anti-cytochrome c, or (**B**) rabbit anti-Bip/GRP78 followed by the appropriate secondary antibodies. Experiments shown are representative confocal images of three to four different experiments performed.

C) GSH in cytosol and mitochondria from chow or ob/ob hepatocytes. Results are expressed as mean ± SD of at least three experiments.

D) Serum ALT and AST levels in ob/ob or lean mice following or not atorvastatin (Atorv) therapy and/or LPS challenge. Data are mean ± SEM. n = 6 mice per group. *$p < 0.05$ versus untreated ob/ob mice; #$p < 0.05$ versus atorvastatin-treated ob/ob mice; **$p < 0.05$ versus LPS-treated ob/ob mice.

E) Representative H&E images from ob/ob mice after atorvastatin therapy or not and/or LPS challenge (magnification at 20×).

these metabolic disturbances are not sufficient for the progression to SH nor for the hepatocellular susceptibility to TNF/Fas, invoking the requirement for additional factors.

Using *NPC1*$^{-/-}$ mice, we show that FC accumulates in hepatocytes in agreement with the observations of extensive unesterified cholesterol storage in the liver of *NPC1*$^{-/-}$ mice (Erickson et al., 2005). Furthermore, we find in both HC-fed rats and *NPC1*$^{-/-}$ mice that FC accumulates in mitochondria, as previously reported in the livers from rats fed a cholesterol-enriched diet (Rogers et al., 1980) or in the brain from *NPC1*$^{-/-}$ mice (Yu et al., 2005). In contrast, FC accumulation in the ER occurs in HC-fed rats as determined in isolated microsomal preparations, but not in hepatocytes from *NPC1*$^{-/-}$ mice, in concordance with previous observations in cholesterol-loaded macrophages from *NPC1*$^{+/-}$ mice (Feng et al., 2003), thus discarding a role for ER stress in contributing to the sensitization to inflammatory cytokines-mediated SH. If the ER FC loading were involved in the hepatocellular susceptibility to TNF, we would expect hepatocytes deficient in NPC1 to be resistant to TNF. Unexpectedly, *NPC1*$^{-/-}$ hepatocytes exhibited an intrinsic susceptibility to TNF, similar to hepatocytes from HC-fed rat liver. Thus, our findings are consistent with the two hits hypothesis, indicating that mitochondrial FC loading but not TG or FFA plays a role as a first hit in the progression of fatty liver disease to SH through sensitization to TNF or Fas.

mGSH depletion and hepatocellular sensitivity to TNF

Our findings reveal the selective depletion of mGSH in both HC-fed rats and *NPC1*$^{-/-}$ mice due to FC loading in mitochondria. Indeed, the mitochondrial transport of GSH is highly sensitive to membrane dynamics and normalization of the mitochondrial membrane fluidity restored the mitochondrial transport of GSH and mGSH levels in cholesterol-enriched mitochondria (Colell et al., 1997; Fernandez-Checa and Kaplowitz, 2005; Lluis et al., 2003). The selective mGSH depletion by HP in normal hepatocytes recapitulated the susceptibility to TNF or Jo2 seen in the HC feeding model or in *NPC1*$^{-/-}$ mice. The question is then: how or why does mGSH determine the hepatocellular susceptibility to TNF? The apoptotic signaling of TNF is complex involving protein-protein interactions and recruitment of signaling mediators that converge on mitochondria that stimulate mitochondrial membrane permeabilization, cytochrome c release, and caspase activation (Bradham et al., 1998; Micheau and Tschopp, 2003). Simultaneously to these death-promoting pathways, TNF activates survival pathways dependent on NF-κB (Kamata et al., 2005; Pham et al., 2004). Our previous studies demonstrated that mGSH depletion with HP enabled TNF to induce cytochrome c release and caspase-3 activation, effects that were preceded by ROS stimulation and prevented by cyclosporin A (Garcia-Ruiz et al., 2003). In addition, we show here that the sensitization of hepatocytes to TNF due to selective mGSH depletion by HP is abrogated by inhibition of caspase 8 and antioxidants. Moreover, our data reveal the requirement of ASMase in TNF-induced oxidative stress and apoptosis in mGSH-depleted hepatocytes, indicating that the mitochondrial ROS generation triggered by TNF and subsequent cell death are dependent on ASMase. Intriguingly, our findings indicate that the sensitization of hepatocytes to TNF by mGSH depletion is not due to NF-κB inactivation, which has been shown to suppress ROS overgeneration and TNF-induced apoptosis (Pham et al., 2004). While enhanced NF-κB DNA binding by TNF occurs early (15–30 min), κB-dependent induction of survival genes may take extra time (hours). In contrast, the ROS generation by TNF in mGSH-depleted hepatocytes occurs very quickly (15–30 min), preceding the upregulation of NF-κB-dependent survival proteins.

FC, mGSH, and NASH

Previous studies reported that alcohol feeding results in mGSH depletion and susceptibility to TNF (Colell et al., 1997, 1998; Wheeler et al., 2001). We extended these observations in NASH, showing mitochondrial FC accumulation, mGSH depletion, and susceptibility to LPS in ob/ob mice. Of relevance, the treatment of ob/ob mice with atorvastatin prevented the FC accumulation in mitochondria and the subsequent mGSH depletion, thus abolishing the susceptibility to LPS-induced liver damage, similar to the findings observed in HC-fed rats treated with SAM. Unlike other statins, the active hydroxy metabolites of atorvastatin, particularly the o-hydroxy derivative, exhibit the same enzymatic inhibition of HMGCoA reductase as the parental statin. In addition, the active o-hydroxy derivative of atorvastatin has been described to prevent cholesterol domain formation by an antioxidant mechanism (Mason et al., 2006). Whether the antioxidant property of this derivative relates to its ability to replenish mGSH levels remains to be established. Enhanced TNF generation in ob/ob mice contributes to NASH as its downregulation by anti TNF antibodies or probiotic therapy has been shown to improve NASH in this model (Li et al., 2003). Recent findings have shown the autoamplification of TNF as a potential mechanism for maintenance of elevated TNF levels (Neels et al., 2006). Hence, the combination of TNF overproduction and mGSH depletion that occur in ob/ob mice are both necessary for SH development. Interestingly, we observed that while atorvastatin corrected the mGSH depletion in ob/ob mice by preventing the mitochondrial FC enrichment, it did not change the TNF overproduction. Because FC accumulation does not perturb TNF signaling as shown in the HC-fed model, the role of FC in promoting TNF sensitization and hence NASH in obese ob/ob mice seems to be mediated through mGSH depletion. The efficacy of atorvastatin in ob/ob mice may further stimulate future clinical studies with statins in patients with NASH.

In conclusion, our findings are consistent with the two-hits hypothesis, with FC accumulation but not TG or FFA playing a key role as a first hit because it sensitizes to inflammatory cytokines-mediated SH through mGSH depletion. Moreover, although TG-loaded livers are resistant to TNF, macrovesicular steatosis and TG may still contribute to NASH development as they can cause hepatic inflammation through NF-κB activation with subsequent TNF generation and adipocytokine unbalance (Cai et al., 2005; Furukawa et al., 2004; Xu et al., 2003). Thus, our findings reveal an unrecognized role of FC in SH and suggest that statins or mGSH-repleting agents may have a niche in the therapeutic armamentarium for SH.

Experimental procedures

Models of hepatic steatosis

Animal studies were approved by the IDIBAPS Animal Care and Use Committee. Male Sprague-Dawley rats (250 g) were fed a choline-deficient methionine sufficient Lombardi diet (Dyets Inc) or its corresponding choline-supplemented control diet, or a hypercholesterolemic diet containing 2% purified cholesterol with or without 0.5% sodium cholate supplementation (Dyets Inc.). *NPC1*$^{-/-}$ and ob/ob mice (both in the C57BL/6 background) were

obtained from The Jackson Laboratories. *ASMase*$^{-/-}$ mice were maintained and used as previously described (Garcia-Ruiz et al., 2003; Mari et al., 2004).

Hepatocyte isolation and mitochondria and microsomal preparation

Hepatocytes were isolated and cultured as described (Garcia-Ruiz et al., 2003; Mari et al., 2004). Rat or mouse hepatocytes were incubated with recombinant human TNF-α (15–280 ng/ml; Peprotech EC). Some cultures were pretreated with the caspase-8 inhibitor Ac-IETD-CHO (50 μM), vitamin E (50 μM), butylated hydroxytoluene (BHT) (100 μM), or GSH-EE (5 mM). For the induction of ER stress, hepatocytes were incubated with tunicamycin (5 μg/ml) plus brefeldin A (10 μg/ml) for 24 hr.

Rat liver mitochondria were isolated by differential centrifugation. Alternatively highly purified mitochondria were prepared by rapid centrifugation through Percoll density gradient as described previously (Colell et al., 2003). Mitochondrial enrichment was ascertained by the specific activity of succinic dehydrogenase, while contamination by ER, plasma membrane, early and recycling endosomes was evaluated by Bip/GRP78, Na^+/K^+ ATPase α1, Rab5A and Rab11 levels, respectively. In addition, acid phosphatase activity monitored the contamination with lysosomes. Mitochondrial integrity was determined by the acceptor control ratio as the ADP-stimulated oxygen consumption over its absence using a Clark oxygen electrode with glutamate/malate or succinate as substrates for respiratory sites for complexes I or II. In some instances, mitochondria were fractionated by digitonin treatment to prepare outer mitochondrial membrane and mitoplasts as described previously (Colell et al., 2003). The efficiency of the procedure was verified by monitoring the monoamine oxidase activity in the low-speed pellet (mitoplasts) compared with the high-speed pellet (outer membrane) or intact mitochondria from the oxidation of benzylamine (3.3 mM final concentration). Hepatic ER fraction was isolated from liver homogenates as described (Ernster et al., 1962) and washed in 0.1 M phosphate buffer (pH 7.2). The activities of glucose-6-phosphatase and succinic dehydrogenase were determined to monitor ER enrichment and purity.

Western blot analyses

Cells were lysed with ice-cold RIPA buffer (1× PBS, 1% NP40, 0.5% sodium deoxycholate, 0.1% SDS), containing 100 μg/mL PMSF and 1× Protease Inhibitor Cocktail Set III (Calbiochem). After centrifugation at 14,000 × g for 30 min, proteins in the supernatants were quantified by the Bradford method (Bio-Rad). Cytosolic, mitochondrial, and nuclear fractions were prepared as previously described (Garcia-Ruiz et al., 2003).

Western Blot analyses were performed using 20–50 μg of protein/lane in 12% denatured polyacrylamide gel and electrophoresed on a nitrocellulose membrane for detection by primary and secondary antibodies. Membranes were incubated with goat polyclonal antibody against Bip/GRP78, rabbit polyclonal anti-caspase 8, goat polyclonal anti-NFκB-p65, mouse monoclonal anti-CHOP/GADD153, rabbit polyclonal anti-β-actin, rabbit polyclonal anti-calreticulin, rabbit polyclonal anti-Rab5A, mouse monoclonal anti-Na^+K^+-ATPase α1 (Santa Cruz Biotechnology), rat monoclonal anti-caspase-12, mouse monoclonal anti-Bax (clone 5B7) (Sigma), mouse monoclonal anti-cytochrome c (clone 6H2.B4; BD Pharmingen), mouse monoclonal anti-Phospho-SAPK/JNK, rabbit polyclonal anti-SAPK/JNK (Cell Signaling Technology), and rabbit polyclonal anti-Rab11 (Zymed). After the incubation with primary antibody, the membrane was washed and incubated with peroxidase-conjugated secondary antibodies (1:5000 dilution; Amersham-Pharmacia), and bound antibody was visualized with ECL detection on Kodak X-OMAT film (Eastman Kodak).

Laser confocal imaging

Cultured rat hepatocytes were fixed for 10 min in 3.7% paraformaldehyde in 0.1 M phosphate buffer prior to permeabilization with 0.1% saponin in 0.5% bovine serum albumin/PBS buffer for 5 min. Cells were incubated for 2 hr with 50 μg/ml filipin, rinsed with PBS-0.0025% saponin, followed by incubation with primary antibodies, mouse anti-cytochrome c antibody (1:500), goat anti-Rab7 polyclonal antibody (1/50), goat polyclonal antibody against Bip/GRP78 (1/50), rinsed with PBS-0.0025% saponin, and incubated for 45 min with secondary antibodies. All steps after the addition of filipin were performed in the dark. After final washes in PBS, cells were mounted and confocal images were collected using a Leica SP2 laser scanning confocal microscope equipped with UV excitation, an argon laser, a 63×/1.32 OIL PH3 CS objective and a confocal pinhole set at 1 Airy unit. All the confocal images shown were single optical sections. Based on the pinhole diameter and instrument settings, the empirical determination of the slice thickness was 479 nm. The number of cells observed per field was at least 70–100 per condition.

Assessment of cell death, liver injury, and myeloperoxidase staining

Hepatocellular cell death following TNF challenge was determined by staining with propidium iodide and Höechst 33258 as described previously (Garcia-Ruiz et al., 2003). Caspase 3 activation from hepatocellular lysates was determined as described (Mari et al., 2004). Liver samples following LPS or Jo2 administration were processed for H&E and myeloperoxidase staining using standard procedures (Servicio Anatomía Patológica, Hospital Clinic).

In vivo LPS-induced steatohepatitis and SAM treatment

Animals were fed the different diets overnight and LPS (5 mg/kg) was given at 8:00 AM next day intravenously, and 3 hr later, SAM was administered (i.p., 15 mg/kg). Animals were sacrificed 24 hr after LPS injection, for histology and serum ALT/AST determinations.

Atorvastatin therapy in ob/ob mice

Male ob/ob and lean mice at 6 weeks of age were maintained under specific pathogen-free condition with controlled temperature and humidity on a 12 hr light-dark cycle. Autoclaved food and water were provided ad libitum. After a 7 day acclimation period, all mice were divided into groups that received either vehicle control (nonpyrogenic water) or atorvastatin. Animals were dosed daily via oral gavage with atorvastatin (10 mg/kg) or vehicle. After 15 days of dosing, mice were killed, and blood and livers were processed for biochemical determinations, TNF measurements, and histology. 24 hr before killing, some mice received an injection intraperitoneally of LPS (0.3 mg/kg).

Statistical analyses

Experiments were performed routinely with at least 4–6 animals per group. Representative data from Western blot or confocal microcopy analyses is shown from at least three independent observations. Statistical comparison of the mean values was performed using Student's t test for unpaired data.

Supplemental data

Supplemental data include Supplemental Experimental Procedures, Supplemental References, and four figures and can be found with this article online at http://www.cellmetabolism.org/cgi/content/full/4/3/185/DC1/.

Acknowledgments

The work presented was supported in part by the Research Center for Liver and Pancreatic Diseases, P50 AA 11999; and grant 1R21 AA014135-01, funded by the US National Institute on Alcohol Abuse and Alcoholism; Plan Nacional de I+D grants SAF (2002-3564, 2003-04974, 2005-03923, 2005-03943, and 2006-0678); and Red Temática de Investigación Cooperativa G03/015, Red de Centros C03/02 PI 05/1285 and FIS (04/1039, 03/0426, 02/3057 and 02/0339) grants supported by Instituto de Salud Carlos III, Spain. The technical assistance of Susana Nuñez is highly appreciated. M.M., A.C., and A.M. are Ramón y Cajal investigators. The authors declare that they have no competing financial interests.

Received: December 22, 2005
Revised: May 9, 2006
Accepted: July 21, 2006
Published: September 5, 2006

References

Abu-Elheiga, L., Brinkley, W.R., Zhong, L., Chirala, S.S., Woldegiorgis, G., and Wakil, S.J. (2000). The subcellular localization of acetyl-CoA carboxylase 2. Proc. Natl. Acad. Sci. USA *97*, 1444–1449.

Angulo, P. (2002). Nonalcoholic fatty liver disease. N. Engl. J. Med. *346*, 1221–1231.

Armstrong, J.S., and Jones, D.P. (2002). Glutathione depletion enforces the mitochondrial permeability transition and causes cell death in Bcl-2 overexpressing HL60 cells. FASEB J. *16*, 1263–1265.

Beltroy, E.P., Richardson, J.A., Horton, J.D., Turley, S.D., and Dietschy, J.M. (2005). Cholesterol accumulation and liver cell death in mice with Niemann-Pick type C disease. Hepatology *42*, 886–893.

Bradham, C.A., Qian, T., Streetz, K., Trautwein, C., Brenner, D.A., and Lemasters, J.J. (1998). The mitochondrial permeability transition is required for tumor necrosis factor alpha-mediated apoptosis and cytochrome c release. Mol. Cell. Biol. *18*, 6353–6364.

Breckenridge, D.G., Germain, M., Mathai, J.P., Nguyen, M., and Shore, G.C. (2003). Regulation of apoptosis by endoplasmic reticulum pathways. Oncogene *22*, 8608–8618.

Brown, M.S., and Goldstein, J.L. (1997). The SREBP pathway: regulation of cholesterol metabolism by proteolysis of a membrane-bound transcription factor. Cell *89*, 331–340.

Browning, J.D., and Horton, J.D. (2004). Molecular mediators of hepatic steatosis and liver injury. J. Clin. Invest. *114*, 147–152.

Brunt, E.M. (2004). Nonalcoholic steatohepatitis. Semin. Liver Dis. *24*, 3–20.

Cai, D., Yuan, M., Frantz, D.F., Melendez, P.A., Hansen, L., Lee, J., and Shoelson, S.E. (2005). Local and systemic insulin resistance resulting from hepatic activation of IKK-beta and NF-kappaB. Nat. Med. *11*, 183–190.

Colell, A., Garcia-Ruiz, C., Lluis, J.M., Coll, O., Mari, M., and Fernandez-Checa, J.C. (2003). Cholesterol impairs the adenine nucleotide translocator-mediated mitochondrial permeability transition through altered membrane fluidity. J. Biol. Chem. *278*, 33928–33935.

Colell, A., Garcia-Ruiz, C., Miranda, M., Ardite, E., Mari, M., Morales, A., Corrales, F., Kaplowitz, N., and Fernandez-Checa, J.C. (1998). Selective glutathione depletion of mitochondria by ethanol sensitizes hepatocytes to tumor necrosis factor. Gastroenterology *115*, 1541–1551.

Colell, A., Garcia-Ruiz, C., Morales, A., Ballesta, A., Ookhtens, M., Rodes, J., Kaplowitz, N., and Fernandez-Checa, J.C. (1997). Transport of reduced glutathione in hepatic mitochondria and mitoplasts from ethanol-treated rats: effect of membrane physical properties and S-adenosyl-L-methionine. Hepatology *26*, 699–708.

Crespo, J., Cayon, A., Fernandez-Gil, P., Hernandez-Guerra, M., Mayorga, M., Dominguez-Diez, A., Fernandez-Escalante, J.C., and Pons-Romero, F. (2001). Gene expression of tumor necrosis factor alpha and TNF-receptors, p55 and p75, in nonalcoholic steatohepatitis patients. Hepatology *34*, 1158–1163.

Erickson, R.P., Bhattacharyya, A., Hunter, R.J., Heidenreich, R.A., and Cherrington, N.J. (2005). Liver disease with altered bile acid transport in Niemann-Pick C mice on a high-fat, 1% cholesterol diet. Am. J. Physiol. Gastrointest. Liver Physiol. *289*, G300–G307.

Ernster, L., Siekevitz, P., and Palade, G.E. (1962). Enzyme-structure relationships in the endoplasmic reticulum of rat liver. A morphological and biochemical study. J. Cell Biol. *15*, 541–562.

Feldstein, A.E., and Gores, G.J. (2005). Apoptosis in alcoholic and nonalcoholic steatohepatitis. Front. Biosci. *10*, 3093–3099.

Feldstein, A.E., Canbay, A., Angulo, P., Taniai, M., Burgart, L.J., Lindor, K.D., and Gores, G.J. (2003). Hepatocyte apoptosis and fas expression are prominent features of human nonalcoholic steatohepatitis. Gastroenterology *125*, 437–443.

Feldstein, A.E., Canbay, A., Giucciardi, M.E., Higuchi, H., Bronk, S.F., and Gores, G.J. (2003b). Diet associated steatosis sensitizes to Fas mediated liver injury in mice. J. Hepatol. *39*, 978–983.

Feng, B., Yao, P.M., Li, Y., Devlin, C.M., Zhang, D., Harding, H.P., Sweeney, M., Rong, J.X., Kuriakose, G., Fisher, E.A., et al. (2003). The endoplasmic reticulum is the site of cholesterol-induced cytotoxicity in macrophages. Nat. Cell Biol. *5*, 781–792.

Fernandez-Checa, J.C., and Kaplowitz, N. (2005). Hepatic mitochondrial glutathione: transport and role in disease and toxicity. Toxicol. Appl. Pharmacol. *204*, 263–273.

Furukawa, S., Fujita, T., Shimabukuro, M., Iwaki, M., Yamada, Y., Nakajima, Y., Nakayama, O., Makishima, M., Matsuda, M., and Shimomura, I. (2004). Increased oxidative stress in obesity and its impact on metabolic syndrome. J. Clin. Invest. *114*, 1752–1761.

Garcia-Ruiz, C., Colell, A., Mari, M., Morales, A., Calvo, M., Enrich, C., and Fernandez-Checa, J.C. (2003). Defective TNF-alpha-mediated hepatocellular apoptosis and liver damage in acidic sphingomyelinase knockout mice. J. Clin. Invest. *111*, 197–208.

Gimpl, G., Burger, K., and Fahrenholz, F. (1997). Cholesterol as modulator of receptor function. Biochemistry *36*, 10959–10974.

Hakamada, K., Sasaki, M., Takahashi, K., Umehara, Y., and Konn, M. (1997). Sinusoidal flow block after warm ischemia in rats with diet-induced fatty liver. J. Surg. Res. *70*, 12–20.

Horton, J.D., Goldstein, J.L., and Brown, M.S. (2002). SREBPs: activators of the complete program of cholesterol and fatty acid synthesis in the liver. J. Clin. Invest. *109*, 1125–1131.

Hotamisligil, G.S. (1999). The role of TNFalpha and TNF receptors in obesity and insulin resistance. J. Intern. Med. *245*, 621–625.

Iimuro, Y., Gallucci, R.M., Luster, M.I., Kono, H., and Thurman, R.G. (1997). Antibodies to tumor necrosis factor alfa attenuate hepatic necrosis and inflammation caused by chronic exposure to ethanol in the rat. Hepatology *26*, 1530–1537.

Ji, C., and Kaplowitz, N. (2004). Hyperhomocysteinemia, endoplasmic reticulum stress, and alcoholic liver injury. World J. Gastroenterol. *10*, 1699–1708.

Kamata, H., Honda, S., Maeda, S., Chang, L., Hirata, H., and Karin, M. (2005). Reactive oxygen species promote TNFalpha-induced death and sustained JNK activation by inhibiting MAP kinase phosphatases. Cell *120*, 649–661.

Kulinski, A., Vance, D.E., and Vance, J.E. (2004). A choline-deficient diet in mice inhibits neither the CDP-choline pathway for phosphatydilcholine synthesis in hepatocytes nor apolipoprotein B secretion. J. Biol. Chem. *279*, 23916–23924.

Lehmann, V., Freudenberg, M.A., and Galanos, C. (1987). Lethal toxicity of lipopolysaccharide and tumor necrosis factor in normal and D-galactosamine-treated mice. J. Exp. Med. *165*, 657–663.

Li, Z., Yang, S., Lin, H., Juang, J., Watkins, P.A., Moser, A.B., DeSimone, C., Song, X., and Diehl, A.M. (2003). Probiotics and antibodies to TNF inhibit inflammatory activity and improve nonalcoholic fatty liver disease. Hepatology *37*, 343–350.

Li, Z., Agellon, L.B., Allen, T.M., Umeda, M., Jewell, L., Mason, A., and Vance, D.E. (2006). The ratio of phosphatidylcholine to phosphatidylethanolamine influences membrane integrity and steatohepatitis. Cell Metab. *3*, 321–331.

Lin, H.Z., Yang, S.Q., Chuckaree, C., Kuhajda, F., Ronnet, G., and Diehl, A.M. (2002). Metformin reverses fatty liver disease in obese, leptin-deficient mice. Nat. Med. *6*, 998–1003.

Liscum, L. (2000). Niemann-Pick type C mutations cause lipid traffic jam. Traffic *1*, 218–225.

Lluis, J.M., Colell, A., Garcia-Ruiz, C., Kaplowitz, N., and Fernandez-Checa, J.C. (2003). Acetaldehyde impairs mitochondrial glutathione transport in HepG2 cells through endoplasmic reticulum stress. Gastroenterology *124*, 708–724.

Mari, M., Colell, A., Morales, A., Paneda, C., Varela-Nieto, I., Garcia-Ruiz, C., and Fernandez-Checa, J.C. (2004). Acidic sphingomyelinase downregulates the liver-specific methionine adenosyltransferase 1A, contributing to tumor necrosis factor-induced lethal hepatitis. J. Clin. Invest. *113*, 895–904.

Mason, R.P., Walter, M.F., Day, C.A., and Jacob, R.F. (2006). Active metabolite of atorvastatin inhibits membrane cholesterol formation by an antioxidant mechanism. J. Biol. Chem. *281*, 9337–9345.

Mavrelis, P.G., Ammon, H.V., Gleysteen, J.J., Komorowski, R.A., and Charaf, U.K. (1983). Hepatic free fatty acids in alcoholic liver disease and morbid obesity. Hepatology *3*, 226–231.

McGarry, J.D., Mannaerts, G.P., and Foster, D.W. (1977). A possible role for malonyl-CoA in the regulation of hepatic fatty acid oxidation and ketogenesis. J. Clin. Invest. *60*, 265–270.

Micheau, O., and Tschopp, J. (2003). Induction of TNF receptor I-mediated apoptosis via two sequential signaling complexes. Cell *114*, 181–190.

Neels, J.G., Pandey, M., Hotamisligil, G.S., and Samad, F. (2006). Autoamplification of tumor necrosis factor-α. A potential mechanism for the maintenance of elevated tumor necrosis factor-α in male but not female obese mice. Am. J. Pathol. *168*, 435–444.

Norman, A.W., Demel, R.A., de Kruyff, B., and van Deenen, L.L. (1972). Studies on the biological properties of polyene antibiotics. Evidence for the direct interaction of filipin with cholesterol. J. Biol. Chem. *247*, 1918–1929.

Osawa, Y., Uchinami, H., Bielawski, J., Schwabe, R.F., Hannun, Y.A., and Brenner, D.A. (2005). Roles for C16-ceramide and sphingosine 1-phosphate in regulating hepatocyte apoptosis in response to tumor necrosis factor-alpha. J. Biol. Chem. *280*, 27879–27887.

Pham, C.G., Bubici, C., Zazzeroni, F., Papa, S., Jones, J., Alvarez, K., Jayawardena, S., De Smaele, E., Cong, R., Beaumont, C., et al. (2004). Ferritin heavy chain upregulation by NF-kappaB inhibits TNFalpha-induced apoptosis by suppressing reactive oxygen species. Cell *119*, 529–542.

Riddle, T.M., Kuhel, D.G., Woollett, L.A., Fichtenbaum, C.J., and Hui, D.Y. (2001). HIV protease inhibitor induces fatty acid and sterol biosynthesis in liver and adipose tissues due to the accumulation of activated sterol regulatory element-binding proteins in the nucleus. J. Biol. Chem. *276*, 37514–37519.

Robin, M.A., Demeilliers, C., Sutton, A., Paradis, V., Maisonneuve, C., Dubois, S., Poirel, O., Letteron, P., Pessayre, D., and Fromenty, B. (2005). Alcohol increases tumor necrosis factor alpha and decreases nuclear factor-kappab to activate hepatic apoptosis in genetically obese mice. Hepatology *42*, 1280–1290.

Ribeiro, P.S., Cortez-Pinto, H., Sola, S., Castro, R.E., Ramalho, R.M., Baptista, A., Moura, M.C., Camilo, M.E., and Rodríguez, C.M. (2004). Hepatocyte apoptosis, expression of death receptors, and activation of NF-kappaB in the liver of nonalcoholic and alcoholic steatohepatitis patients. Am. J. Gastroenterol. *99*, 1708–1717.

Rogers, K.S., Higgins, E.S., and Grogan, W.M. (1980). Influence of dietary cholesterol on mitochondrial function in the rat. J. Nutr. *110*, 248–254.

Rouslin, W., MacGee, J., Gupte, S., Wesselman, A., and Epps, D.E. (1982). Mitochondrial cholesterol content and membrane properties in porcine myocardial ischemia. Am. J. Physiol. *242*, H254–H259.

Shan, X., Jones, D.P., Hashmi, M., and Anders, M.W. (1993). Selective depletion of mitochondrial glutathione concentrations by (R,S)-3-hydroxy-4-pentenoate potentiates oxidative cell death. Chem. Res. Toxicol. *6*, 75–81.

Soccio, R.E., and Breslow, J.L. (2004). Intracellular cholesterol transport. Arterioscler. Thromb. Vasc. Biol. *24*, 1150–1160.

Tilg, H., and Diehl, A.M. (2000). Cytokines in alcoholic and nonalcoholic steatohepatitis. N. Engl. J. Med. *343*, 1467–1476.

Tomita, K., Tamiya, G., Ando, S., Ohsumi, K., Chiyo, T., Mizutani, A., Kitamura, N., Toda, K., Kaneko, T., Horie, Y., et al. (2006). Tumour necrosis factor a signaling through activation of Kupffer cells plays an essential role in liver fibrosis of non-alcoholic steatohepatitis in mice. Gut *55*, 415–424.

Uysal, K.T., Wiesbrock, S.M., Marino, M.W., and Hotamisligil, G.S. (1997). Protection from obesity-induced insulin resistance in mice lacking TNF-alpha function. Nature *389*, 610–614.

Van Blitterswijk, W.J., Van Hoeven, R.P., and Van der Meer, B.W. (1981). Lipid structural order parameters (reciprocal of fluidity) in biomembranes derived from steady-state fluorescence polarization measurements. Biochim. Biophys. Acta *644*, 323–332.

Werstuck, G.H., Lentz, S.R., Dayal, S., Hossain, G.S., Sood, S.K., Shi, Y.Y., Zhou, J., Maeda, N., Krisans, S.K., Malinow, M.R., and Austin, R.C. (2001). Homocysteine-induced endoplasmic reticulum stress causes dysregulation of the cholesterol and triglyceride biosynthetic pathways. J. Clin. Invest. *107*, 1263–1273.

Wheeler, M.D., Nakagami, M., Bradford, B.U., Uesugi, T., Mason, R.P., Connor, H.D., Dikalova, A., Kadiiska, M., and Thurman, R.G. (2001). Overexpression of manganese superoxide dismutase prevents alcohol-induced liver injury in the rat. J. Biol. Chem. *276*, 36664–36672.

Williams, K., Rao, Y.P., Natarajan, R., Pandak, W.M., and Hylemon, P.B. (2004). Indinavir alters sterol and fatty acid homeostatic mechanisms in primary rat hepatocytes by increasing levels of activated sterol regulatory element-binding proteins and decreasing cholesterol 7alpha-hydroxylase mRNA levels. Biochem. Pharmacol. *67*, 255–267.

Woo, C.W., Siow, Y.L., Pierce, G.N., Choy, P.C., Minuk, G.Y., Mymin, D., and O, K. (2005). Hyperhomocysteinemia induces hepatic cholesterol biosynthesis and lipid accumulation via activation of transcription factors. Am. J. Physiol. Endocrinol. Metab. *288*, E1002–E1010.

Xu, A., Wang, Y., Keshaw, H., Xu, L.Y., Lam, K.S., and Cooper, G.J. (2003). The fat-derived hormone adiponectin alleviates alcoholic and nonalcoholic fatty liver diseases in mice. J. Clin. Invest. *112*, 91–100.

Yin, M., Wheeler, M.D., Kono, H., Bradford, B.U., Gallucci, R.M., Luster, M.I., and Thurman, R.G. (1999). Essential role of tumor necrosis factor alpha in alcohol-induced liver injury in mice. Gastroenterology *117*, 942–952.

You, M., and Crabb, D.W. (2004). Molecular mechanisms of alcoholic fatty liver: role of sterol regulatory element-binding proteins. Alcohol *34*, 39–43.

Yu, W., Gong, J.S., Ko, M., Garver, W.S., Yanagisawa, K., and Michikawa, M. (2005). Altered cholesterol metabolism in Niemann-Pick type C1 mouse brains affects mitochondrial function. J. Biol. Chem. *280*, 11731–11739.